



Bedload transport controls bedrock erosion under sediment-starved conditions

A. R. Beer^{1,2} and J. M. Turowski^{1,3}

¹WSL Swiss Federal Institute for Forest, Snow and Landscape Research, 8903 Birmensdorf, Switzerland

²Department of Environmental System Sciences, ETH Zurich, 8092 Zurich, Switzerland

³GFZ German Research Centre for Geosciences, Telegrafenberg, 14473 Potsdam, Germany

Correspondence to: A. R. Beer (alexander.beer@wsl.ch)

Received: 2 December 2014 – Published in Earth Surf. Dynam. Discuss.: 6 January 2015

Revised: 26 May 2015 – Accepted: 8 June 2015 – Published: 13 July 2015

Abstract. Fluvial bedrock incision constrains the pace of mountainous landscape evolution. Bedrock erosion processes have been described with incision models that are widely applied in river-reach and catchment-scale studies. However, so far no linked field data set at the process scale had been published that permits the assessment of model plausibility and accuracy. Here, we evaluate the predictive power of various incision models using independent data on hydraulics, bedload transport and erosion recorded on an artificial bedrock slab installed in a steep bedrock stream section for a single bedload transport event. The influence of transported bedload on the erosion rate (the “tools effect”) is shown to be dominant, while other sediment effects are of minor importance. Hence, a simple temporally distributed incision model, in which erosion rate is proportional to bedload transport rate, is proposed for transient local studies under detachment-limited conditions. This model can be site-calibrated with temporally lumped bedload and erosion data and its applicability can be assessed by visual inspection of the study site. For the event at hand, basic discharge-based models, such as derivatives of the stream power model family, are adequate to reproduce the overall trend of the observed erosion rate. This may be relevant for long-term studies of landscape evolution without specific interest in transient local behavior. However, it remains to be seen whether the same model calibration can reliably predict erosion in future events.

1 Introduction

Quantitative landscape evolution analysis is a fundamental domain in today’s geomorphological research. The hydrological system plays an important role in landscape response to tectonics through the formation of drainage networks, the adjustment of river channel shape and slope, and the routing of sediments (e.g., Howard et al., 1994; Whipple and Tucker, 1999; Whipple, 2004). Thus, a mechanistic understanding of the processes that are active in rivers and their mathematical description is crucial in order to capture landscape evolution as a whole (e.g., Lague, 2014). Bedrock rivers are particularly frequent in mountainous regions and there have been many attempts to model their erosional work (overviews by Sklar and Dietrich, 2006; Turowski, 2012; Whipple et al., 2013). A number of physical fluvial erosion processes acting on bedrock surfaces have been described, and abrasion

by bedload and plucking of blocks are thought to be the most important of these (cf. Whipple et al., 2013). Both processes are driven by the impact of bedload particles on the bedrock surface.

Bedrock incision is generally thought to depend on flow hydraulics and in situ substrate properties. This notion forms the basis of the most commonly used erosion models of the stream power incision model family (Howard and Kerby, 1983; Seidl et al., 1994; Turowski, 2012; Lague, 2014), in which erosion rate is a power function of stream power or bed shear stress (Whipple and Tucker, 1999). However, mechanistically, it is known that fluvial bedrock incision is driven by the impact of sediment particles (Sklar and Dietrich, 2001; Hartshorn et al., 2002; Turowski, 2012; Cook et al., 2013; Turowski et al., 2015). Several effects of the transported sediment need to be accounted for. These are the “thresholds of motion and suspension” that are related to a characteristic

grain size (Lague et al., 2003; Sklar and Dietrich, 2004; Attal et al., 2011), the shielding of bedrock by sediments, known as the “cover effect” (e.g., Gilbert, 1877; Turowski et al., 2008; Johnson et al., 2009), and erosive pebble impacts on the bedrock that depend on the amount of mobile sediment, known as the “tools effect” (e.g., Foley, 1980; Turowski and Rickenmann, 2009; Cook et al., 2013). Taking into account these four effects, erosion rate E can be written as (cf. Sklar and Dietrich, 2006)

$$E = K H_y^a S_e^b F_e^c Q_s^d. \quad (1)$$

Here, the scaling of bedrock erodibility, sediment erosivity and, consequently, the dominant erosional process, are lumped together in a model-specific prefactor K (e.g., Howard, 1994; Sklar and Dietrich, 2006). H_y is a placeholder for an effective hydraulic parameter (e.g., discharge, stream power, bed shear stress), in which the term efficient means it can incorporate a threshold of grain motion. Thus, H_y represents the sediment motion effects in these cases. The suspension effect term S_e is the fraction of particles in suspension, F_e is the fraction of bed exposure, which is related to the cover effect, and Q_s is the sediment transport rate, describing the availability of erosive tools (see Appendix A for more details). The exponents a , b , c , and d modulate the dependence of erosion rate on these four effects, respectively.

Available fluvial erosion models were originally developed at the process scale, and their application to whole stream sections or even catchments is problematic (e.g., Lague et al., 2005). Spatial upscaling, from process to reach scale, and from reach to catchment scale, is not completely understood. Several factors should be taken into account explicitly, such as time (Gardner et al., 1987; Mills, 2000; Finnegan et al., 2014), space (Hancock et al., 1998; Wohl, 1998; Goode and Wohl, 2010), changing morphology (Inoue et al., 2014; Johnson, 2014; Zhang et al., 2015), and variability in forcing conditions, such as discharge, climate or sediment process interactions (Hancock et al., 1998; Snyder et al., 2003; Lague et al., 2005; Whipple et al., 2013). In addition, many models predict similar steady-state morphology (e.g., Whipple and Tucker, 2002; Lague, 2014), but the transient evolution of entire channels is difficult to reconstruct in the field, and hence model validation is challenging.

The theoretical consideration of incision model sensitivity (Sklar and Dietrich, 2006) and model assessment by means of field data have, to date, largely focused on the steady-state geometry of entire channels (Lague, 2014). van der Beek and Bishop (2003) remodeled the long-profile evolution of incising rivers in the Upper Lachlan catchment (southeastern Australia) based on known paleo-profiles. They found that all of the tested models gave reasonable predictions for the current long profiles with the application of suitable parameter sets. In contrast, Tomkin et al. (2003) determined that none of the tested models could satisfactorily explain the data from the well-studied Clearwater River (northwestern

Washington State, USA), which is thought to exhibit steady-state incision. Tomkin et al. (2003), however, attributed this failure more to the quality of their data, rather than to the inadequacy of the applied incision models. A different approach was taken by Turowski et al. (2013, 2015), who compared field measurements of energy delivery to the streambed to predictions using the saltation–abrasion model (Sklar and Dietrich, 2004). This approach, however, can only be applied to specific model types because only one of the model’s elements is compared to field data.

The problem of model adequacy and potential study-site sensitivity can be simplified if models and their behavior are examined at the process scale (Whipple and Tucker, 1999; Tucker and Whipple, 2002). However, such evaluations have not been possible to date due to the lack of data at the appropriate resolution (Turowski, 2012). Hence, the transient validity of fluvial erosion models at the process scale has neither been assessed in the laboratory nor in the field. Here, we use field data of unprecedented detail and quality (Beer et al., 2015) to directly evaluate available fluvial incision models at the process scale, using a transient bedrock erosional signal throughout a single sediment transport event. Thus, we obtain constraints for the modeling of fluvial bedrock erosion at a scale that has not been studied previously.

2 Observation site and data

The Erlenbach is a small pre-Alpine mountain stream in Switzerland that hosts a well-instrumented bedload transport observatory. In 2011, the site was supplemented with a novel setup for measuring bedrock erosion, which was named “erosion scales” (Beer et al., 2015). The infrastructure, measurement methods, and accuracy have been described in detail elsewhere (Rickenmann et al., 2012; Turowski et al., 2013; Beer et al., 2015), and are only briefly summarized here. Discharge is gauged with 15 % uncertainty, bedload mass transport (henceforth referred to as bedload transport) can be determined to an accuracy of $1 \text{ kg} \pm 30 \%$ using the Swiss plate geophone bedload sensor system (here called the geophone sensor), and at-a-point erosion sensors in the streambed have a resolution of better than 0.1 mm with 5 % uncertainty. The measurements of these three quantities are completely independent and all data are recorded at a time resolution in minutes (Beer et al., 2015).

For the following analysis, we study a rainfall-induced discharge event at the Erlenbach stream, featuring a peak flow of $1.1 \text{ m}^3 \text{ s}^{-1}$ with strong supercritical and turbulent flow conditions (the mean Froude number is 6.7 and the Reynolds number exceeds 10^5 ; Fig. 1, Table 1). The entire investigation period (termed “event period” in Fig. 1) starts at the onset of the stream’s response to rainfall and ends some hours after the rainfall, broadly defining a time frame around the actual bedload transport event. We focus on the surface erosion measured on a dry-packed concrete slab (a test “bedrock”) placed

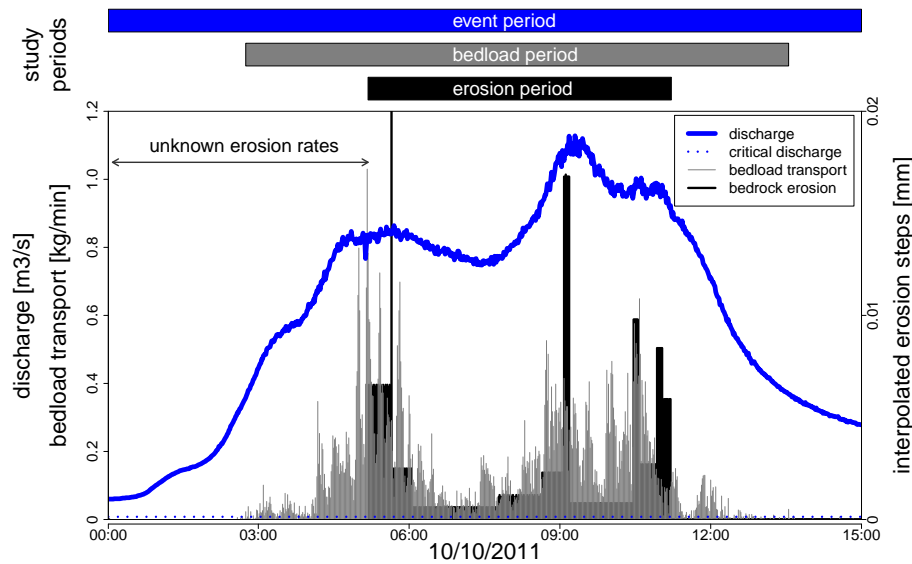


Figure 1. Overview of the erosive discharge event showing the three independently measured data sets. The colored bars on top indicate the three study periods for model sensitivity analysis.

flush against the streambed of an artificially fixed smooth chute channel with a slope of 16%. This chute channel is attached to a natural alluvial streambed section upstream that is shallower and is characterized by a high macro-roughness in the form of step-pool units and isolated boulders (Yager et al., 2012a, b). Thus, the broader setting represents a convex knickpoint transition from an alluvial to a bedrock streambed with a length of around 30 m, situated upstream from the measurement installation. The concrete bedrock slab was overpassed by 8.8 t of bedload in nearly 11 h, as detected by the geophone sensor located immediately downstream (Rickmann et al., 2012; Beer et al., 2015). The slab hosts three vertical at-a-point erosion sensors that continuously record surface elevation. In addition, the slab was surveyed with close-range photogrammetry (Rieke-Zapp et al., 2012) before and after the event to confirm the measured cumulative erosion rates at the erosion sensor positions.

Here, we restrict our analysis to erosion sensor c3, which was located in the middle of the flow path and featured the highest erosion rate (cf. Beer et al., 2015). The sensor recorded 13 erosion steps during the event, with a total erosion of 0.85 mm. The temporal evolution of erosion before the first recorded step is unknown. Hence, only subsequent data are used for analysis (termed “erosion period” in Fig. 1). To account for the temporal uncertainty of the occurrence of the individual erosion steps and to obtain a transient curve, we use linearly interpolated data, hereafter referred to as c3i. The course of this curve is a robust representation of the erosional evolution of the sensor and its cumulative value is consistent with the erosive pattern of the surrounding slab surface (cf. Beer et al., 2015).

The chute channel streambed approaching the erosion sensor c3 shows a 8 m wide trapezoidal cross section of jointed rip-rap with low bed roughness (the standard deviation of streambed elevations is 0.04 m). In any case, using an at-a-point sensor, the spatial scale of the erosion measurement is small. Hence, bed morphology or roughness does not have a strong influence on the erosion signal and the flow properties are homogeneous on the site of the sensor. These facts, together with its steeper slope compared to the natural channel upstream, cause sediment-starved or detachment-limited conditions in the chute channel. Overall, the situation at the measurement site is close to the conditions that are typically assumed in process-scale erosion models, and specifically to those for the derivation of the saltation–abrasion model (Sklar and Dietrich, 2004).

3 Methods

Our purpose is to assess the ability of erosion models to predict observed transient bedrock erosion c3i (linearly interpolated data from the erosion sensor c3). Sklar and Dietrich (2006) classified the spectrum of existing incision models according to their incorporation of the four types of sediment effects (Eq. 1). We selected a representative model from each of their classes (Table 2). These models are (I) unit stream power USP, (II) excess unit stream power EUSP, (III) linear decline LD, (IV) alluvial bedload AB, (V) tools T, (VI) parabolic stream power SPP, (VII) the saltation–abrasion model neglecting the suspension effect SAws, and (VIII) the saltation–abrasion model including the suspension effect SA. In addition, we included a variant of T, a tools-only dependent model TO (Va), in which erosion rate is propor-

Table 1. Event statistics. Values are given for the event period, unless otherwise indicated.

Data	Value
Site data	
Local bed slope	16 %
Bed roughness (standard deviation of bed elevations)	0.04 m
event data	
Length of event period	900 min
Length of bedload period	649 min
Length of erosion period	363 min
Total discharge	33'095 m ³
Maximum discharge	1.1 m ³ s ⁻¹
Range of water depth	0.01–0.17 m
Range of stream width	0.53–2.43 m
Event bedload grain size d_{30} (30 vol% grains are smaller)	0.015 m
Event bedload grain size d_{50} (50 vol% grains are smaller)	0.020 m
Event bedload grain size d_{90} (90 vol% grains are smaller)	0.075 m
Total bedload transported ^a	8.8 t
Total at-a-point erosion of erosion sensor c3	0.85 mm
Observed at-a-point erosion steps	13
Bedload motion (H_y)	
Calculated critical shear stress (Shields stress)	0.006
Critical discharge	0.008 m ³ s ⁻¹
Critical shear stress	1.9 N m ⁻²
Critical unit stream power	5.9 W m ⁻²
Mean Froude number	6.7 ± 3.3
Range of Reynolds numbers	10 ⁵ –10 ⁶
Range of Rouse numbers	3.0–13.1
Mean transport stage τ_s (shear stress/critical shear stress)	75 ± 38
Mean relative bedload supply (actual bedload/potential bedload) ^b	0.07 ± 0.07
Maximum relative bedload supply	0.56
Mean bedload concentration (bedload/discharge) ^b	0.006 ± 0.006
Maximum bedload concentration	0.05
Bedload suspension (S_e)	
Mean suspension term S_e	0.64 ± 0.18
Minimum suspension effect S_e	0.34
Bedrock exposure (F_e)	
Mean fraction of exposure F_e	0.95 ± 0.07
Minimum fraction of exposure F_e	0.44
Bedload transport (Q_s)	
Maximum bedload transport Q_s	103 kg min ⁻¹
Mean bedload transport ^b Q_s	14 kg min ⁻¹

^a Over a bed area of 0.18 m² surrounding the erosion sensor (the concrete slab).

^b Values for the bedload period.

tional to cumulated bedload transport rate (see Appendix A for model details). To evaluate the predictive quality of these models against a standard, we further used the simplest possible model as a null hypothesis that assumes a constant erosion rate during the entire period of consideration: (H0) con-

stant erosion. Note that a model based on stream power can be converted into a model based on shear stress and vice versa using simple assumptions of hydraulic geometry and flow velocity (cf. Whipple and Tucker, 1999). Thus, models

Table 2. The applied incision models. The second horizontal line subdivides models that include the tools effect from models that do not. The notation of variables in the explicit models is given in Appendix A.

Model class ¹	Model name ¹	Original reference	Considered sediment effects ²				General model shape ³	Explicit model ⁴
			Motion	Susp.	Cover	Tools		
H0	Constant erosion						$E \sim 1/(\text{length of period})$	$E \sim 1/(\text{length of period})$
I	Unit stream power (USP)	Howard et al. (1994)	–	–	–	–	$E \sim H_y^a$	$E \sim \omega^a$
II	Excess unit stream power (EUSP)	Sklar and Dietrich (2006)	✓	–	–	–	$E \sim H_{yex}^a$	$E \sim \omega_{ex}^a$
III	Linear decline (LD)	Whipple and Tucker (2002)	–	–	✓	–	$E \sim H_y^a F_c^c$	$E \sim \omega^a (1 - Q_s/Q_{sc})^c$
IV	Alluvial bedload (AB)	Sklar and Dietrich (2006)	✓	–	✓	–	$E \sim H_{yex}^a F_c^c$	$E \sim \tau_{ex}^a (1 - Q_s/Q_{sc})^c$
Va	Tools only (TO) ⁵	This work	–	–	–	✓	$E \sim Q_s^d$	$E \sim Q_s^d$
V	Tools (T)	Foley (1980)	✓	–	–	✓	$E \sim H_{yex}^a Q_s^d$	$E \sim \tau_{ex}^a Q_s^d$
VI	Parabolic stream power (SPP)	Whipple and Tucker (2002)	–	–	✓	✓	$E \sim H_y^a F_c^c Q_s^d$	$E \sim \omega^a (1 - Q_s/Q_{sc})^c Q_s^d$
VII	Saltation–abrasion without suspension (SAws)	Sklar and Dietrich (2006)	✓	–	✓	✓	$E \sim H_{yex}^a F_c^c Q_s^d$	$E \sim \tau_{ex}^a (1 - Q_s/Q_{sc})^c Q_s^d$
VIII	Saltation–abrasion (SA)	Sklar and Dietrich (2004)	✓	✓	✓	✓	$E \sim H_{yex}^a S_e^b F_c^c Q_s^d$	$E \sim \tau_{ex}^a (1 - u^*/w_f)^b (1 - Q_s/Q_{sc})^c Q_s^d$

¹ Based on the classification by Sklar and Dietrich (2006); model choice and description is given in Appendix A.

² Grain motion and suspension thresholds, cover and tools effects.

³ Based on Eq. (1).

⁴ Based on Eq. (A1).

⁵ Concept of this work.

USP and EUSP can be seen as representative of other members of the stream power model family.

Recently published models dealing with the interplay between bed roughness and sediment cover regarding erosion rates (Johnson, 2014; Inoue et al., 2014; Zhang et al., 2015) were not considered here. This is because the channel at the experimental site features a steep and smooth bed downstream from a rougher and shallower bed. This resulted in low relative sediment supply (maximum 0.56) and bedload concentrations with high transport stages (given the low mean grain size d_{50}), and therefore high fractions of exposure (Table 1). Consequently, sediment–roughness interactions and bed cover are unlikely. We furthermore did not explicitly apply the elaborate total-load model by Lamb et al. (2008a), due to its need for high shear stress ratios combined with high relative sediment supply to deviate from the SAws model (Lamb et al., 2008a; Scheingross et al., 2014), which is not the case at the Erlenbach stream. Models focusing on plucking as the dominant erosion process (Chatanantavet and Parker, 2009; Dubinski and Wohl, 2013) were also not considered since abrasion can be assumed to be the dominant process in our experimental setting (cf. Beer et al., 2015). For further details on model choice and parametrization, see Appendix A.

The threshold of bedload motion on site was calculated based on Rickenmann et al.’s equation for the critical discharge in steep torrent channels (see Eq. 18 in Rickenmann et al., 2006), and resulted in a very low value of $0.008 \text{ m}^3 \text{ s}^{-1}$. This threshold was far exceeded during the entire study period (cf. Fig. 1), and corresponds to a critical Shields stress of 0.006, i.e., a nondimensionalized version of the bed shear stress used for the initiation of particle motion (cf. Shields, 1936; Table 1). The calculated value is below the commonly applied lower limit of 0.03 (e.g., Buffington and Montgomery, 1997; Sklar and Dietrich, 2004) and an order of magnitude lower than that calculated with an empirical equation for steep alluvial streams (0.09; Lamb et al., 2008b, Fig. 1 therein). However, the standard deviation of bed el-

evations in the vicinity of the erosion sensor c3 is 0.04 m (Table 1), implying a smooth bedrock surface, for which a critical Shields stress of 0.006 is plausible (cf. Hodge et al., 2011; Chatanantavet et al., 2013; Auel, 2014). This value is also consistent with no visual observations of sediment deposits (neither sand nor cobbles) in the chute channel section and on top of the geophones over many years. Thus, the prevailing transport stage, defined as the ratio of acting nondimensional bed shear stress over critical Shields stress, was generally high.

As is apparent from Fig. 1, actual bedload transport started after the exceedance of the calculated threshold of motion, at least for the particle sizes that are detectable with the geophone sensors ($> 0.01 \text{ m}$; cf. Rickenmann et al., 2012). This is due to the fact that the detachment of the bedload passing on site actually occurred in the upstream natural stream section under completely different hydraulic conditions (cf. Turowski et al., 2011, 2013; Yager et al., 2012a, b). There, the relative importance of the four sediment effects presumably is different from the measurement site, and the threshold of bedload motion is higher (cf. Schneider et al., 2014). Since we focus on the chute channel, it would not be plausible to use a threshold of motion from the alluvial section. However, to assess its downstream influence on bedload transport and for the assessment of the motion effect, we defined an additional virtual threshold of bedload motion (VTBM) at the observed exceedance of a bedload transport rate of 1 kg min^{-1} (which is the beginning of the bedload period; cf. Fig. 1), corresponding to a critical discharge of $0.36 \text{ m}^3 \text{ s}^{-1}$, a critical unit stream power of 407 W m^{-2} and a critical Shields stress of 0.26.

We calculated erosion rates with each model for the flood event under consideration using independently observed hydraulic parameters and sediment transport rates. The relationships between discharge, flow height, and stream width that are required for the calculation of hydraulic parameters such as local unit stream power at the position of the observed bedrock slab were determined using the methods described

Table 3. Exponents of the four sediment effects (cf. Eq. 1) for the common (com) and optimized (opt) model versions, respectively, given for the three simulation time periods under consideration and the resulting model performance relative to c3i. Implausible parameters are indicated in bold and model groups with and without the tools effect are separated by a horizontal line.

Model period	Model name ^a	Applied model parameters ^b								Model performance	
		Motion		Suspension		Cover		Tools		RMSE _{com} (%)	RMSE _{opt} (%)
		a _{com}	a _{opt}	b _{com}	b _{opt}	c _{com}	c _{opt}	d _{com}	d _{opt}		
	Const. ero. (H0)									12	
Event period	USP (class I)	0.5 ^c	1.5 ^c	–	–	–	–	–	–	10	8
	EUSP (class II)	0.5	1.5	–	–	–	–	–	–	10	8
	LD (class III)	2.0 ^c	2.5 ^c	–	–	1.0	–5.6	–	–	9	4
	AB (class IV)	1.5	2.8	–	–	1.0	–5.6	–	–	9	4
	TO (class Va)	–	–	–	–	–	–	1.0	1.0	3	3
	T (class V)	–0.5	0.6	–	–	–	–	1.0	1.0	5	3
	SPP (class VI)	1.0 ^c	–0.4 ^c	–	–	1.0	1.6	1.0	1.3	5	3
	SAws (class VII)	–0.5	–0.5	–	–	1.0	1.6	1.0	1.3	3	3
	SA (class VIII)	–0.5	26	1.5	24	1.0	1.6	1.0	1.2	6	3
		Const. ero. (H0)									10
Bedload period	USP (class I)	0.5 ^c	1.1 ^c	–	–	–	–	–	–	9	8
	EUSP (class II)	0.5	1.0	–	–	–	–	–	–	9	8
	LD (class III)	2.0 ^c	2.3 ^c	–	–	1.0	–5.4	–	–	10	4
	AB (class IV)	1.5	2.6	–	–	1.0	–5.4	–	–	9	4
	TO (class Va)	–	–	–	–	–	–	1.0	1.0	4	4
	T (class V)	–0.5	0.6	–	–	–	–	1.0	1.0	5	4
	SPP (class VI)	1.0 ^c	–0.4 ^c	–	–	1.0	1.6	1.0	1.3	6	4
	SAws (class VII)	–0.5	–0.5	–	–	1.0	1.6	1.0	1.3	4	4
	SA (class VIII)	–0.5	26	1.5	24	1.0	1.6	1.0	1.2	6	3
		Const. ero. (H0)									11
Erosion period	USP (class I)	0.5 ^c	0.0 ^c	–	–	–	–	–	–	11	11
	EUSP (class II)	0.5	0.0	–	–	–	–	–	–	11	11
	LD (class III)	2.0 ^c	2.3 ^c	–	–	1.0	–8.3	–	–	13	5
	AB (class IV)	1.5	2.5	–	–	1.0	–8.3	–	–	12	5
	TO (class Va)	–	–	–	–	–	–	1.0	2.3	7	5
	T (class V)	–0.5	–0.5	–	–	–	–	1.0	1.7	6	5
	SPP (class VI)	1.0 ^c	–1.8 ^c	–	–	1.0	2.6	1.0	2.3	11	5
	SAws (class VII)	–0.5	–2.1	–	–	1.0	2.7	1.0	2.3	8	5
	SA (class VIII)	–0.5	31	1.5	24	1.0	– 14	1.0	–1.0	7	5

^a Model denotations are given in Table 2.

^b Respective parameters for commonly used (_com) and optimized (_opt) values applied for the four sediment effects.

^c This exponent is used for entire stream power neglecting the grain motion threshold effect.

by Beer et al. (2015). The mean grain size of the transported sediment during the event considered here was estimated at 0.02 m (using data by Rickenmann et al., 2012, Fig. 9 therein) at a mean discharge of $0.77 \text{ m}^3 \text{ s}^{-1}$ and a mean bedload transport rate of $0.45 \text{ kg m}^{-1} \text{ s}^{-1}$ for the period of observed bedload transport. During the event, bedrock abrasion apparently was the dominant erosional process, since neither direct observations nor surveying results gave any indication of solution, plucking or cavitation (Beer et al., 2015).

The interpolated erosion line c3i and the individual model outcomes were scaled to unity to focus on transient behavior, ignoring the prefactors K with their multivariate sensitivities to lithology, climate, and sediment (Whipple and Tucker, 1999). Since we only have reliable erosion data some time after the onset of bedload transport (cf. Fig. 1), we calcu-

lated model performance sensitivity on bedload transport using three separate simulation time periods. For the “event period”, the start and end of the simulation were set at arbitrary times broadly including the studied bedload transport event. For the “bedload period”, the start and end of the simulation period coincide with the observed bedload transport period as measured with the geophone sensor, while the “erosion period” only covers the time span where c3i data exist.

For the evaluation of the transient individual model performance, overall deviations between model predictions and c3i were quantified by means of the root mean square error (RMSE; cf. van der Beek and Bishop, 2003; Valla et al., 2010) of the cumulative values, and minute-by-minute differences were considered in order to assess model feasibility and highlight dominant processes. The proportion of

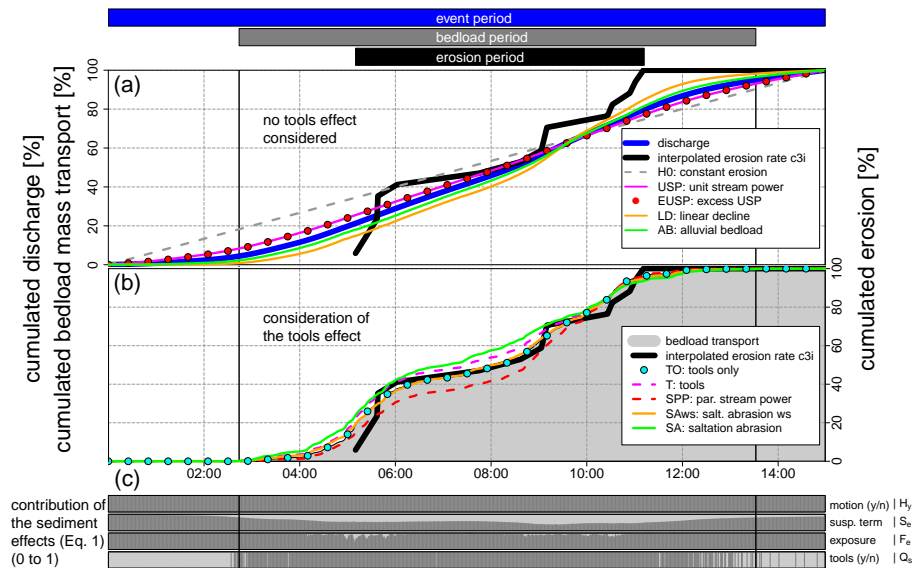


Figure 2. Evolution of the modeled erosion signals over the flood event compared to discharge, bedload mass transport and interpolated erosion rate (see Table 2 and Appendix A for model descriptions) given for the event period. Positions of all three simulation time periods are shown on top like in Fig. 1. **(a)** Scaled predictions of constant erosion and models neglecting the tools effect (models USP to AB), **(b)** scaled predictions for models incorporating the tools effect (models TO to SA) and **(c)** the transient evolution of the four sediment effects (factors in Eq. 1; data resolution is in minutes). Note that the threshold of motion term and the tools term are binary, but the suspension term and the fraction of exposure term can continuously vary between 0 and 1; see text for further explanations.

explained variance PEV (a measure commonly known as the Nash–Sutcliffe model efficiency coefficient in hydrology; e.g., Gyalistras, 2003) was used as a second measure to evaluate model predictive quality, utilizing instantaneous rather than cumulative erosion values. In addition, we optimized individual model performance by adjusting the exponents a , b , c , and d (see Eq. 1), as long as they differed from 0, to minimize the RMSE based on the methods of Brent (1973) and Nelder and Mead (1965). We are aware of the fact that the exponents of the saltation–abrasion model SA (Sklar and Dietrich, 2004) and some of the exponents in other models come from physics-based analyses. Similarly, bedrock erosion can be expected to be linearly dependent on sediment supply due to the tools effect (cf. Sklar and Dietrich, 2001, 2004; Johnson and Whipple, 2010; Whipple et al., 2013; Auel, 2014; Jacobs and Hagmann, 2015). However, we decided to consider all models as implementations of a generic model equation (Eq. 1 or the more detailed Eq. A1; see Appendix A) and therefore analyzed their performance with optimized exponents despite potential mechanistic parametrizations.

4 Results

All incision models performed at least slightly better than the null hypothesis of constant erosion (Fig. 2, Table 3). The tested models can be roughly separated into two groups based on their transient behavior, corresponding to those models that do and those that do not include the tools effect

Q_s (Fig. 2a and b). Here, we focus on the event period to describe the main observations. A detailed comparison of each model in each simulation time period is given in Appendix B (Fig. B1).

The models of the first group (models USP to AB; Fig. 2a; Table 2) show a smooth increase in cumulative erosion over the course of the event, while those of the second group (models TO to SA; Fig. 2b) exhibit a wavy pattern. With respect to the four sediment effects, we observed the following.

- i. Threshold of motion: due to the small value of this threshold, it was exceeded during the whole study period and there is no effect visible (e.g., no difference between USP and EUSP). All models in Fig. 2a predicted erosion even when none was detected (cf. Sklar and Dietrich, 2006), which is particularly obvious at the end of the observation period where $c3i$ data are available. However, applying the higher virtual threshold VTBM at the actual onset of bedload transport (i.e., restriction of the scaled model evolution to the limits of the bedload period with $H_y = 0$ outside the vertical lines in Fig. 2c) led to a smoother fit of models EUSP and AB to $c3i$ (not shown here). Hence, inclusion of a threshold of motion is of distinct importance, especially if the tools effect is ignored.
- ii. Threshold of suspension: the status of complete suspension transport (this corresponds to $S_e = 0$) was not reached during this event for grain sizes equal to or

greater than 0.02 m (cf. Fig. 2c). The mean of the suspension term S_e (for details on the calculation, see Appendix A) was 0.64 ± 0.18 throughout the event, with a minimum of 0.34 (Table 1), and thus substantial pebble saltation was predicted. The use of model SA that includes the suspension effect term showed a larger deviation from the data than the otherwise equivalent model SAws (Fig. 2b).

- iii. Cover effect: the fraction of exposure F_e average was 0.95 ± 0.07 with a minimum value of 0.44. Hence, there was no time when erosion was completely prohibited (Fig. 2c) and consequently there was no remarkable improvement in modeling performance when including the cover term, e.g., when comparing models USP and LD (Fig. 2a).
- iv. Tools effect: the wavy pattern observed in the erosion record c3i, as well as in the models that include the tools effect (TO to SA; Fig. 2b), closely follows the evolution of cumulative bedload transport over the course of the event with model SPP showing the largest deviation. Actual bedload transport Q_s initiated at VTBM here, but it receded before falling below this threshold again at the end of the event period. This recession is accompanied by the cessation of the continued increase in c3i.

Models including the tools effect (TO to SA, Fig. 2b) show smaller RMSE than those that do not for all three simulation time periods, except model SPP using the standard parameter set and applied during the erosion period (Table 3). All model predictions except for model TO improved when optimized, with the highest improvements for the erosion period (in this period, also TO). However, for model SA, the optimized exponents of both threshold factors (motion and suspension) show implausible values. For all other models, exponents only adjusted moderately during optimization.

Analysis of the minute-by-minute differences of each model prediction from c3i (Fig. 3a) revealed the same pattern of a noticeable improvement for models that include the tools effect (cf. RMSE values from Table 3 in Fig. 3b), since models neglecting it (USP–AB) did not perform better than the null hypothesis of constant erosion. Remarkably, this pattern is also visible in the PEV values (Fig. 3c), which are based on the instantaneous erosion values that show greater variability. A PEV value < 0 means poor model performance, since $PEV = 0$ modeling is comparable to the assumption of constant erosion and > 0 indicates a reduced error variance compared to variance in the original values of c3i (cf. Gyalistras, 2003).

Generally, for both the event period and the bedload period we obtained similar results, while for the erosion period models showed comparably worse predictions (cf. Fig. B2). Models neglecting the tools effect underpredicted observed erosion by 7 and 4% (median) for the first two simulation time periods (both for the common and optimized param-

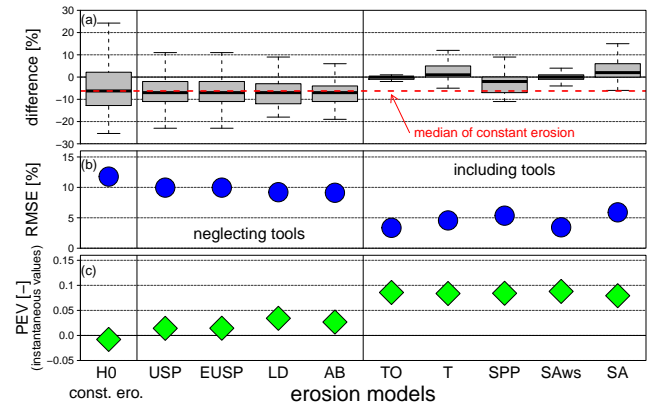


Figure 3. Comparison of individual model performance for the event period: (a) prediction differences from the course of bedrock erosion c3i, (b) root mean square errors RMSE and (c) proportion of explained variances PEV (calculated for the instantaneous erosion values). For model denotations, see Table 2.

ter sets), whereas models including the tools effect showed medians of differences of nearly 0%. For the erosion period the median values were partially better, but the interquartile ranges were larger by far. The interquartile ranges of the models SAws and SA showed the smallest values when using the optimized parameter in the event period, but their overall performance is comparable to the TO model. Model SPP, which neglects the threshold of motion, had the worst performance of all approaches that consider bedload tools, when standard parameters were used. Model parameter optimization achieved the most improvements for the erosion period, where the performance of models that include the tools effect could be improved to a quality comparable to that achieved in the two other simulation time periods using standard parameter sets (Fig. B2, Table 3).

5 Discussion

5.1 Model sensitivity to simulation time period

Incision model behavior was comparable for the event period and for the bedload. For the erosion period, the performance of all models was notably worse than in the other periods as visible from the largely increased interquartile ranges of the model differences per minute (Table 3 and Fig. B2). However, the worsened performance is an artifact of scaling all erosion series to 1 for the model evaluation. In contrast to both of the other periods, in which cumulated erosion rate c3i actually started at the first certain erosion step (i.e., > 0) within the time period under consideration, analysis for the erosion period began with c3i set to 0 to ensure a common initiation of all variables. Thus, any erosion that occurred before the beginning of the erosion period was disregarded. With $R^2 = 0.96$, the strength of the correlation between c3i and the cumulative bedload during the erosion period is

slightly smaller than for the event period and the bedload period ($R^2 = 0.98$ for both), and this smaller correlation translates directly to the predictive power of the tools effect for measured erosion. The decreased correlation strength may have various causes. (i) If the bedload path in the channel bed systematically changes as discharge increases, the correlation between bedload transport rates and erosion rates may decrease, since small discharges were omitted in the erosion period. (ii) Bedload transport rates are measured over the entire slab surface (0.18 m^2), but the erosion sensor records at-a-point. (iii) The erosion sensor does not measure continuously, but in steps. Therefore, temporal variability in pebble impacts can cause mismatches between bedload transport rates and erosion rates. (iv) Due to the shorter period of interest, and to the scaling of the total erosion rate to 1, the sharp increase in $c3i$ around 05:40 (Fig. 1) resulted in higher relative deviations of the incision models.

Nevertheless, the pattern of model improvement by including the tools effect was the same for all simulation time periods. In addition, the RMSE values are reasonably similar for all three time periods, both for the common and the optimized model versions. Hence, at least for the timescales investigated here, there is no significant temporal sensitivity to model application regarding actual bedload transport.

5.2 Relevance of the four sediment effects

In the following, we evaluate the predictive power of the four sediment effects in the same order as given in the section on results.

i. The inclusion of the negligible threshold of bedload motion (cf. Table 1) did not have any effect on model performance. However, application of the virtual motion threshold VTBM led to a smoother match between the models EUSP and AB with the observations compared to models USP and LD. Even though the details in the transient pattern of erosion could not be reproduced with these models, the inclusion of the VTBM threshold enabled the prediction of the general observed trend, at least for this event. Thus, as has been previously suggested (cf. Lague et al., 2003; Chatanantavet et al., 2013; Lague, 2014), the inclusion of a threshold of motion is necessary to obtain a plausible temporal pattern of erosion. Therefore, if no direct information on bedload transport is available, the threshold of motion in H_y might be the most relevant parameter for erosion modeling (cf. Sklar and Dietrich, 2006; Attal et al., 2011). Furthermore, as has already been argued in sediment transport studies (e.g., Rickenmann and Koschni, 2010), while the local threshold of motion might not be relevant on site, the threshold of the channel section upstream that is actually supplying the sediment may be. This threshold can be used as a virtual discharge thresh-

old to determine the timing and the amount of bedload transport at the site of interest.

- ii. Within the data set analyzed here, the inclusion of the suspension effect term decreased the predictive quality of the SA model compared to the otherwise equivalent model SAs that does not include it. Increasing the suspension threshold in the suspension effect term S_e (cf. Eq. A1) was not reasonable due to the already high values of the fraction of exposure F_e . In contrast, threshold values below 0.65 (i.e., the maximum of the squared term in the S_e term) prohibited erosion predictions at high shear velocities when actual erosion in $c3i$ occurred. Together with high Rouse numbers (cf. Table 1), this indicates that the bedload transport mode for the mean grain size d_{50} was likely dominant during this event, even with the high transport stages prevailing (75 ± 38). The scaling here is different: while bed shear stress scales linearly with flow depth, shear velocity scales with the square of flow depth and discharge velocity was nearly constant during the event period at $4\text{--}5.6 \text{ ms}^{-1}$. The suspension term proposed by Sklar and Dietrich (2004) could not be evaluated here in more detail, but its lack of explanatory power is consistent with the assumption of Lamb et al. (2008a), who extended the SA model to account for erosion by suspended load due to turbulence-driven impacts. However, as discussed above, the total erosion model of Lamb et al. (2008a) would not substantially deviate from the SA model here, since relative bedload supply was very low (cf. Table 1).
- iii. Explicit consideration of the cover effect is recommended in the literature (e.g., Lamb et al., 2008a; Nelson and Seminara, 2011; Whipple et al., 2013). However, the influence of bed cover (in the form of the F_c term) appears to be insignificant here. Given the site characteristics, the absence of the cover effect is plausible. Due to the increased transport capacity of the chute channel compared to the natural streambed upstream, relative sediment supply was low and the mean transported sediment size d_{50} was lower than the situation on site would allow. Hence, detachment-limited conditions prevailed (cf. Turowski et al., 2013; Beer et al., 2015) and sediment deposition did not occur. This means that static cover did not occur and that dynamic cover (cf. Turowski et al., 2007) was unlikely.
- iv. Erosion rate $c3i$ smoothly followed the accumulated bedload transport during the event period (cf. Fig. 2b). This indicates that erosion is driven by particle impacts and that the dominant sediment effect was the tools effect. Therefore, a simple empirical model in which the erosion rate is proportional to bedload transport rate Q_s (the TO model) explains the data similarly to and as well as other models that incorporate the tools effect (Fig. 3,

Table 3), including highly developed mechanistic process models such as the full saltation–abrasion model (SA). The importance of the tools effect, and its linear dependency on bedload volume, is in line with previous field and laboratory observations (Sklar and Dietrich, 2001; Turowski and Rickenmann, 2009; Cook et al., 2013; Wilson et al., 2013; Auel, 2014; Jacobs and Haggmann, 2015), and our data provide the first direct field evidence for the tools effect at the process scale at high temporal resolution (cf. Whipple et al., 2013; Beer et al., 2015).

5.3 Optimized model parameters

For some models, the optimization procedure resulted in substantial improvements in their predictive power. Because of its considerable practical importance, we discuss the behavior of the stream power incision model family (USP) in detail, and make some general remarks on other models, especially those where we found large predictive differences between the common and optimized parameters.

For the USP model, the optimized exponent a on unit stream power ω was 1.5 for the event period and 1.1 for the bedload period (Table 3). However, the choice of this exponent did not significantly affect the predictive power of the models (Fig. 4), at least when it remained within the range of values reported in the literature (between 0 and 2; see Lague, 2014, for a review). For the modeling with the higher threshold of motion VTBM, the optimized parameter a of the EUSP model was 0.6, close to the common value of 0.5. Both of these numbers support the common usage. However, our observations at the process scale are not directly comparable to previously published values, which are typically derived from measurements at the reach or catchment scale. A proper upscaling and a comparison with reach-scale measurements would be necessary to enable a complete interpretation of these results. For the USP model, we obtained an optimized value of a close to 0 for the erosion period, but with no noticeable improvement over the common parameter of 0.5 (Table 3). To summarize, at least for the specific case of the chute channel and the studied event at the Erlenbach stream, the inclusion of a motion threshold in the USP equation (the EUSP model) makes the common parameter value of 0.5 acceptable for the modeling of the general trend in the transient evolution of bedrock erosion.

Model optimization for all three simulation time periods led to negative values for the exponents of the fraction of exposure F_e for models LD and AB. This resulted in a comparably good performance for the two models, since the first “hump” in the $c3i$ curve could be predicted (cf. Fig. 2 at around 05:30). However, the cover effect was negligible in the setting at hand and a negative exponent value for F_e contradicts the physical assumptions of the cover effect (see Appendix A) since it increased the value of this factor and,

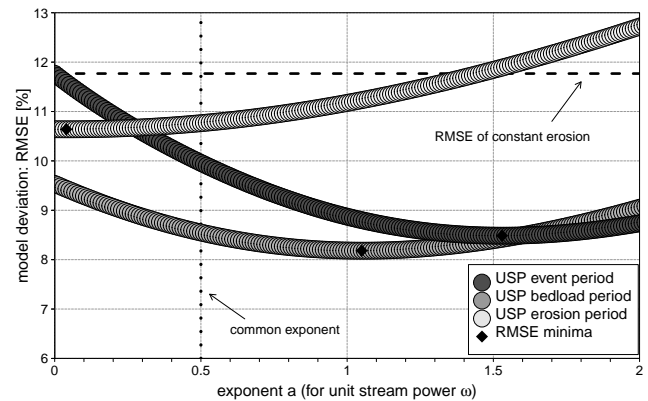


Figure 4. Performance of the USP model expressed as RMSE deviation from measured erosion $c3i$ for the common range of the unit stream power exponent a (increments of 0.1) for the three time periods. The dotted vertical line indicates the commonly used exponent of 0.5; the diamonds show optimized parameters and the dashed line is the RMSE value of constant erosion (model HO) for the event period.

therefore, resembled the tools effect. The observation thus underlines the importance of erosive tools.

Parameter optimization for models TO to SA in part led to a strong nonlinear dependency of the erosion rate on the tools effect (cf. Table 3), together with negative exponent values a for H_y and partly increased exponent values c for F_e . As mentioned above, this can be related to an adjustment of the model curve to predict the first “hump” in the $c3i$ curve (cf. Fig. B1). This short period of higher erosion rates can be traced back to two subsequent erosion steps measured with the erosion sensor $c3$ (cf. Fig. 1; Beer et al., 2015, Fig. 5 therein). Since overall bedload transport at this time was rather below average and comparable bedload transport rates otherwise caused lower spatial surface erosion, the steps may likely be related to a high-energy strike of a single bedload grain at the precise position of the at-a-point erosion sensor. Hence, the nonlinearity here was rather a confirmation than a falsification of the process physics, i.e., that erosion is proportional to the sediment impact energy (cf. Sklar and Dietrich, 2004). Furthermore, the tendency to optimize the parameter d towards values exceeding 1 implies the absence of a dynamic cover effect, for which $d < 1$ would be expected, at least in the TO model. Finally, the implausibly high values of the optimized exponents for model SA in comparison to the otherwise equivalent model SAs may be related to the fact that the definition of the suspension term might be incorrect (see discussion above). The common exponents of the reduced model SAs are physics based, and therefore optimization was not very effective. This might indicate that the basic physics of bedrock erosion is fairly well captured by the saltation–abrasion model. Similarly, Turowski et al. (2013, 2015) found that the hydraulic forcing of the energy delivery

to the bed, which is thought to be proportional to the erosion rate, is well captured by the SA model.

Overall, optimizing of models that include the tools effect mainly resulted in reductions of the interquartile ranges of model deviations. Values for the event period and the bedload period were equally adjusted. Notable improvement, leading to a similar performance in comparison to the other models, was achieved in the SPP model, where the tools effect compensated for the missing threshold of bedload motion. However, no model could clearly beat the performance of the simple TO model (cf. Fig. 3), which is the most effective indicator that the tools effect is the dominant driver of bedrock erosion in our setup.

5.4 Generality of the results

Our results thus far are only based on a single erosive event with regard to a mean sediment grain size. For analysis, the start and end of the event were more or less fixed and the erosion rate was scaled to 100%. Thus, model performance was generally good. However, differences in individual performances were visible and could be used to evaluate governing effects.

The specific situation of a steep smooth bedrock section downstream from an alluvial channel resulting in detachment-limited conditions makes the Erlenbach stream site ideally suited for the study of the tools effect, which is the dominant erosion effect here. We confirmed the linear dependence of bedrock abrasion on bedload flux (as expected by Whipple et al., 2013) using independent transient field data at a temporal resolution in minutes. This supports the assumption that erosion is driven by particle impacts (e.g., Sklar and Dietrich, 2001, 2004; Turowski et al., 2013). Deviations from linear scaling are plausible over the given sediment size distribution, with larger grains showing higher impact energy efficiencies and smaller grains showing lower ones, which can be related to differing transport modes (Turowski et al., 2015). However, focusing on the mean grain size d_{50} seemed to average out these relationships, and the simple TO model was shown to be sufficient to predict bedrock erosion under the given conditions.

For comparable situations where mean values of bedload volumes and erosion rate on bare bedrock sections are available, this model can be easily calibrated by adjusting its prefactor K . Potential applications are steep bedrock channels in detachment-starved catchments (e.g., Wohl, 1998, 1999), channel knickpoint sections with exposed bedrock such as waterfalls (e.g., Miller, 1991; Wohl et al., 1994; Cook et al., 2013; Mackey et al., 2014; DiBiase et al., 2015), high lateral bedrock sections above the channel or its banks (e.g., Hartshorn et al., 2002; Turowski et al., 2008) or even hydropower facilities that have to cope with natural sediment flux such as sediment bypass tunnels (Jacobs and Hagmann, 2015).

Models of the commonly applied stream power model family USP were still found to be feasible, which is important due to the rarity of measured bedload transport rates. The excess unit stream power incision model EUSP using the common exponent of 0.5 was shown to be adequate to reproduce the tools-dominated incision, if the details of erosional evolution within the events are not of interest. However, to define the effective threshold of motion and the characteristic grain size, it is crucial to recognize the streambed situation upstream, which restricts the timing and magnitude of erosion on site.

Inherent channel morphology (e.g., Wohl, 1998; Johnson and Whipple, 2010) crucially steers the dominance of the tools effect for whole-stream evolution and linked landscape evolution in terms of bed roughness (Inoue et al., 2014; Johnson, 2014), relative sediment supply (Turowski et al., 2008; Lague, 2010), transport mode (Lamb et al., 2008a; Scheingross et al., 2014; Turowski et al., 2015), and lithology (Sklar and Dietrich, 2001; Whipple et al., 2013). Thus, the cover effect gains importance (Turowski et al., 2007) and a more complex model such as SAws should be suitable. For the USP model family, at least some aspects of temporal upscaling are understood (e.g., Lague et al., 2005). However, our understanding of spatial upscaling in general, and of temporal upscaling of sediment-flux-dependent incision models specifically, is unclear to date (cf. Whipple and Tucker, 1999; Lague, 2010, 2014).

The model-specific prefactors K (cf. Eq. 1) could be calibrated by scaling the absolute cumulative model predictions with the observed cumulative erosion rate c_{3i} . These factors are partly empirical (e.g., for the USP model) or are based on known material properties (e.g., in the SA model; for an overview, see Sklar and Dietrich, 2006). Analysis of these values, however, is not the focus here, and would need to take more events into consideration for a robust calibration on site.

6 Conclusions

Fluvial bedrock erosion is driven by the impacts of sediment particles. Out of several sediment effects, the tools effect dominantly determines erosion rates at the Erlenbach stream erosion observatory, which exemplifies a steep bedrock channel downstream of an alluvial streambed. The pattern of transient erosion during the course of a single flood event can be described by a simple model in which erosion rate is proportional to bedload transport. Moreover, this simple model performs similarly well or better than more complex models from the literature, including the mechanistically based saltation–abrasion model, and several models from the stream-power incision model family. The model can be site calibrated with temporally lumped data, and is applicable in, for example, detachment-limited steep and smooth bedrock

rivers, in bedrock knickpoint reaches as well as in bedload-exposed hydropower infrastructure.

On the scale of the individual event, models from the stream-power incision model family can adequately describe the generally observed erosion trend. In our tests, the application of an excess shear stress model with an exponent of 0.5 does not capture the detailed evolution of erosion throughout the event, but is adequate to represent the overall form of the erosion curve, if it is parameterized with an adjusted threshold of bedload motion. Analysis of more events is needed to verify whether this result can be generalized, or whether it is specific to the event and field site considered here. Additional data acquisition and analysis of transient erosion rates in other settings are required (Tucker and Whipple, 2002) to, for example, study interactions between different erosion processes that are not considered in modeling to date (Whipple et al., 2013), to examine the model-specific prefactors K , and to potentially provide guidance for site-specific model choice based on locally active morphological processes.

Appendix A: Model selection

According to Sklar and Dietrich (2006), all fluvial bedrock incision models published to date can be represented by a generic equation (a detailed version of Eq. 1):

$$E = K (H_y - H_{yc})^a \left[1 - \left(\frac{u^*}{w_f} \right)^2 \right]^b \left(1 - \frac{Q_s}{Q_{sc}} \right)^c (Q_s)^d. \quad (\text{A1})$$

Here, H_y represents transport stage ts (the fraction of nondimensional bed shear stress and nondimensional critical Shields stress) or unit stream power ω . H_{yc} is a potentially associated threshold term accounting for grain motion, which results in excess transport stage ts_{ex} and excess unit stream power ω_{ex} (given as H_{yex} in Table 2). Q_{sc} is sediment transport capacity, u^* is flow shear velocity and w_f is particle fall velocity in still water for the mean grain size d_{50} . The terms in brackets from the left to the right represent the bedload motion effect, the bedload suspension effect, and the fraction of bedrock exposure (referring to the cover effect) and the tools effect, respectively (cf. Eq. 1).

There are $2^4 = 16$ combinations of the four sediment effects controlled by the exponents a , b , c and d in an incision model, that in turn can be adjusted for specific dominant erosion processes such as abrasion, plucking and macroabrasion (Whipple et al., 2000; Sklar and Dietrich, 2004; Lamb et al., 2008a; Chatanantavet and Parker, 2009; Dubinski and Wohl, 2013). We restricted our analysis to the eight model classes (i.e., combinations of sediment effect parameters) identified by Sklar and Dietrich (2006) that were proposed, analyzed and applied in several studies to date, but added a null hypothesis model (class H0) and a simple bedload-dependent model (class Va). We analyzed one representative of each bedrock incision model class whose selection (Table 2) and parameterization (Table 3) were based on the following reasons (cf. Sklar and Dietrich, 2006).

- Class H0, constant erosion: this model served as a null hypothesis (H0) and simply assumes a constant erosion rate over the time period considered. The fixed instantaneous erosion rate equaled the cumulated erosion rate at the end of the period (i.e., 1, since it was scaled) divided by the length of the period.
- Class I, unit stream power model (USP): this model (Seidl and Dietrich, 1992; Howard, 1994; Howard et al., 1994) is most widely used in landscape evolution modeling studies (Lague, 2014) and for the interpretation of channel long profiles (e.g., Braun and Willett, 2013), although there is evidence contradicting its predictions (Gasparini et al., 2007; Lague, 2014). It is straightforward since it only incorporates discharge data, neglects any sediment effects, and assumes $H_{yc} = 0$. The single exponent a to scale unit stream power ω (which is proportional to discharge) is mainly set to 0.5 in modeling studies as done in the present study, but may vary between 0 and 2 for field data (Croissant and Braun, 2014; Lague, 2014), and most field cases suggest $a = 1$ (e.g., Stock and Montgomery, 1999; Snyder et al., 2000; see Lague, 2014, for a review). The USP model is equivalent to the shear stress model (Howard and Kerby, 1983; Turowski, 2012) and their model exponents are related by a factor of 2/3 (Whipple and Tucker, 1999).
- Class II, excess unit stream power model (EUSP): an extended version of the USP model with non-zero H_{yc} (Sklar and Dietrich, 2006), thus incorporating a threshold of unit stream power to permit grain motion. Here, we applied the excess unit stream power ω_{ex} with the calculated unit stream power value at the onset of bedload motion (cf. Table 1) using the same model exponent $a = 0.5$ as in the USP model (e.g., Tucker and Slingerland, 1997; Whipple et al., 2000).
- Class III, linear decline model (LD): this model set was formulated by Whipple and Tucker (2002) and is functionally equivalent to the undercapacity model by Beaumont et al. (1992). However, the latter does not draw on the cover effect. Instead, it draws on the consumption of discharge energy for sediment transport that would otherwise be used for erosion. Erosion rate is limited by the fraction of actual bedload Q_s to bedload transport capacity Q_{sc} , i.e., the cover effect. If this fraction approaches 1, erosion decreases to 0 (Sklar and Dietrich, 2004). The exponential dependency of the cover term proposed by Turowski et al. (2007) was not applied due to the prevailing tools domain. We applied the bedload transport equation of Rickenmann (2001, Eq. 3 therein) to calculate Q_{sc} with a prefactor calibrated for the Erlenbach stream, using a grain size fraction d_{90}/d_{30} based on data by Rickenmann et al. (2012, Fig. 9 therein; cf. Table 1). We restricted our analysis to the model version of Whipple and Tucker (2002) with an exponent $a = 2$.
- Class IV, alluvial bedload (AB): Sklar and Dietrich (2006) proposed this version of the linear decline model LD, based on excess transport stage ts_{ex} and accounting for the threshold of motion $H_{yc} = 1$.
- Class Va, tools-only model (TO): this model simply relates the erosion rate to the observed cumulative bedload transport rate. We introduce it here with the tools exponent $d = 1$ (based on, e.g., Sklar and Dietrich, 2001; Jacobs and Hagmann, 2015) and rank it into the classification of Sklar and Dietrich (2006), based on the top-down introduction system of the sediment effects there.
- Class V, tools (T): the model of Foley (1980) was applied following the approximation given by Sklar and Dietrich (2006) using $a = -0.5$.

- Class VI, parabolic stream power (SPP): in their attempt to include both the tools and the cover effect, Whipple and Tucker (2002) developed this model based upon considerations of Sklar and Dietrich (1998) using unit stream power ω . We chose the proposed version with $a = 1$.
- Class VII, saltation–abrasion model without the suspension effect (SAws): the same model as SPP, but using excess transport stage t_{sex} instead of unit stream power ω and additionally incorporating the sediment motion threshold H_{yc} .
- Class VIII, full saltation–abrasion model (SA): the complete saltation–abrasion model (Sklar and Dietrich, 2004) additionally accounts for the grain suspension effect. We adopted the threshold of ceasing erosion (1 in the suspension term; Eq. A1) from Sklar and Dietrich (2004); however, this value is controversial (cf. the review by Cheng and Chiew, 1999), and indeed the whole conception has been questioned (Lamb et al., 2008a; Scheingross et al., 2014). The parameter b responsible for the suspension term was set to 1.5 here, since this is consistent with the original model (cf. Sklar and Dietrich, 2004).

Appendix B: Detailed model results

The individual parameter sets of all incision models (USP to SA) were optimized for the three simulation time periods, respectively (Table 3). In Fig. B1, a separate comparison of transient model behavior is shown for the particular model predictions compared to the observed erosion course c3i. For further visual assessment of the individual model performance, the transient model differences from c3i for all three periods are provided as boxplots without whiskers in Fig. B2.

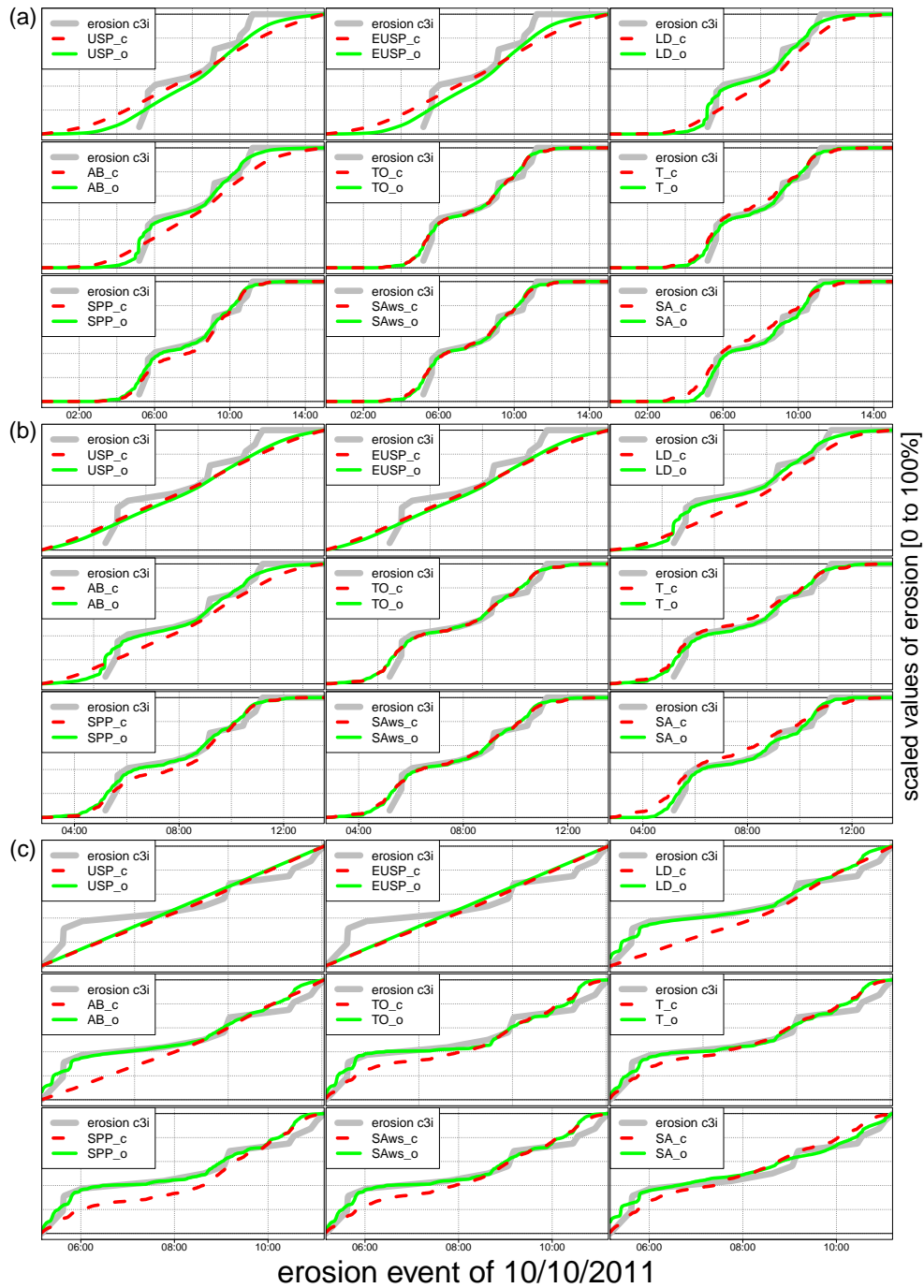


Figure B1. Separate comparison of each of the model-based erosion predictions to c3i for (a) the event period, (b) the bedload period and (c) the erosion period using the individual common and optimized parameter sets, respectively.

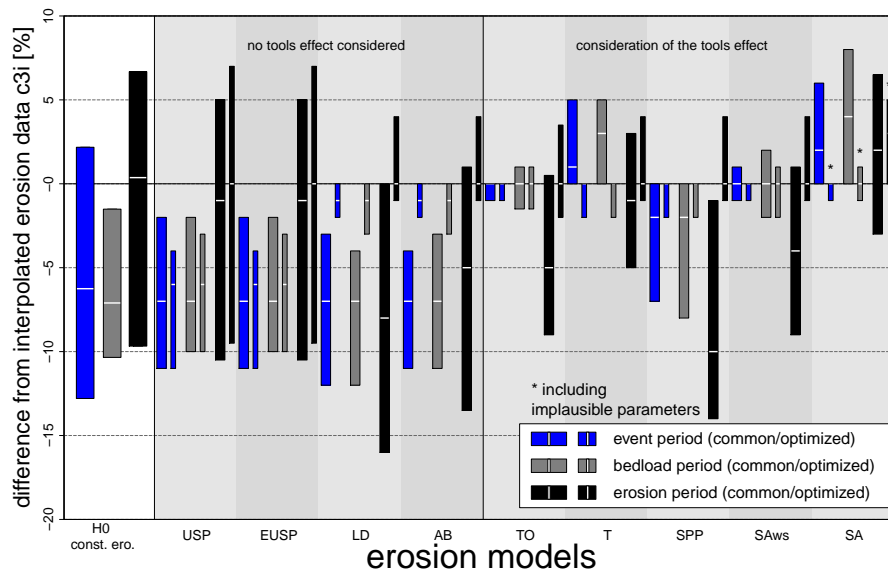


Figure B2. Separate comparison of the differences between model predictions and c3i given as boxplots (without outliers). Each model performance is shown for the three different periods of consideration (the same colors as the time periods indicated in Figs. 1 and 2) with runs using both common and optimized parameter sets (wide and narrow boxes) for each model.

Acknowledgements. The authors are grateful to Florian Heimann, James Kirchner, Joel Scheingross, Colin Stark and Carlos Wyss for fruitful discussions and help with data analysis. Comments by Alexandre Badoux and Johannes Schneider on an earlier version greatly improved the text. The authors are further thankful to an anonymous referee, Phairot Chatanantavet and Leonard Sklar for their thorough reviews, helpful comments and hints. We thank Curtis Gautschi for valuable suggestions that helped to improve the language of an earlier version of the manuscript. This study was supported by SNF grant 200021_132163/1.

Edited by: E. Lajeunesse

References

- Attal, M., Cowie, P. A., Whittaker, A. C., Hobley, D., Tucker, G. E., and Roberts, G. P.: Testing fluvial erosion models using the transient response of bedrock rivers to tectonic forcing in the Apennines, Italy, *J. Geophys. Res.*, 116, F02005, doi:10.1029/2010JF001875, 2011.
- Auel, C.: Flow Characteristics, Particle Motion and Invert Abrasion in Sediment Bypass Tunnels, *Mitteilungen*, in: *Laboratory of Hydraulics, Hydrology and Glaciology (VAW), Mitteilungen* 229, edited by: Boes, R. M., ETH Zurich, 2014.
- Beaumont, C., Fullsack, P., and Hamilton, J.: Erosional control of active compressional orogens, in: *Thrust tectonics*, edited by: McClay, K., Chapman and Hall, New York, 1–18, 1992.
- Beer, A. R., Turowski, J. M., Fritschi, B., and Rieke-Zapp, D.: Field instrumentation for high-resolution parallel monitoring of bedrock erosion and bedload transport, *Earth Surf. Proc. Land.*, 40, 530–541, doi:10.1002/esp.3652, 2015.
- Braun, J. and Willett, S. D.: A very efficient $O(n)$, implicit and parallel method to solve the stream power equation governing fluvial incision and landscape evolution, *Geomorphology*, 180, 170–179, doi:10.1016/j.geomorph.2012.10.008, 2013.
- Brent, R. P.: *Algorithms for Minimization without Derivatives*, Prentice-Hall, Englewood Cliffs, N.J., 1973.
- Buffington, J. M. and Montgomery, D. R.: A Systematic Analysis of Eight Decades of Incipient Motion Studies, with Special Reference to Gravel-Bedded Rivers, *Water Resour. Res.*, 33, 1993–2029, doi:10.1029/96WR03190, 1997.
- Chatanantavet, P. and Parker, G.: Physically-based modeling of bedrock incision by abrasion, plucking, and macroabrasion, *J. Geophys. Res.*, 114, F04018, doi:10.1029/2008JF001044, 2009.
- Chatanantavet, P., Whipple, K. X., Adams, M. A., and Lamb, M. P.: Experimental study on coarse grain saltation dynamics in bedrock channels, *J. Geophys. Res.-Earth*, 118, 1161–1176, doi:10.1002/jgrf.20053, 2013.
- Cheng, N. S. and Chiew, Y. M.: Analysis of initiation of sediment suspension from bed load, *J. Hydraul. Eng.-ASCE*, 125, 855–861, doi:10.1061/(ASCE)0733-9429(1999)125:8(855), 1999.
- Cook, K. L., Turowski, J. M., and Hovius, N.: A demonstration of the importance of bedload transport for fluvial bedrock erosion and knickpoint propagation, *Earth Surf. Proc. Land.*, 38, 683–695, doi:10.1002/esp.3313, 2013.
- Croissant, T. and Braun, J.: Constraining the stream power law: a novel approach combining a landscape evolution model and an inversion method, *Earth Surf. Dynam.*, 2, 155–166, doi:10.5194/esurf-2-155-2014, 2014.
- DiBiase, R. A., Whipple, K. X., Lamb, M. P., and Heimsath, A. M.: The role of waterfalls and knickzones in controlling the style and pace of landscape adjustment in the western San Gabriel Mountains, California, *Geol. Soc. Am. Bull.*, 127, 539–559, doi:10.1130/B31113.1, 2015.
- Dubinski, I. M. and Wohl, E.: Relationships between block quarrying, bed shear stress, and stream power: a physical model of block quarrying of a jointed bedrock channel, *Geomorphology*, 180, 66–81, doi:10.1016/j.geomorph.2012.09.007, 2013.
- Finnegan, N. J., Schumer, R., and Finnegan, S.: A signature of transience in bedrock river incision rates over timescales of 10(4)–10(7) years, *Nature*, 505, 391–394, doi:10.1038/nature12913, 2014.
- Foley, M. G.: Bedrock incision by streams: summary, *Geol. Soc. Am. Bull.*, Part II, 91, 2189–2213, doi:10.1130/0016-7606(1980)91<577:BIBSS>2.0.CO;2, 1980.
- Gardner, T. W., Jorgensen, D. W., Shuman, C., and Lemieux, C. R.: Geomorphic and tectonic process rates – effects of measured time interval, *Geology*, 15, 259–261, doi:10.1130/0091-7613(1987)15<259:GATPRE>2.0.CO;2, 1987.
- Gasparini, N. M., Whipple, K. X., and Bras, R. L.: Predictions of steady state and transient landscape morphology using sediment-flux-dependent river incision models, *J. Geophys. Res.*, 112, F03S09, doi:10.1029/2006JF000567, 2007.
- Gilbert, G. K.: *Land sculpture, The Geology of the Henry Mountains*, Chapter V, United States Department of the Interior, Washington, DC, 99–155, 1877.
- Goode, J. R. and Wohl, E.: Substrate controls on the longitudinal profile of bedrock channels: implications for reach-scale roughness, *J. Geophys. Res.-Earth*, 115, F03018, doi:10.1029/2008JF001188, 2010.
- Gyalistras, D.: Development and validation of a high-resolution monthly gridded temperature and precipitation data set for Switzerland (1951–2000), *Clim. Res.*, 25, 55–83, doi:10.3354/cr025055, 2003.
- Hancock, G. S., Anderson, R. S., and Whipple, K. X.: Beyond power: bedrock river incision process and form, in: *Rivers Over Rock: Fluvial Processes in Bedrock Channels*, edited by: Tinkler, K. J. and Wohl, E. E., Geophysical Monograph, 107, American Geophysical Union, Washington, DC, 30–60, 1998.
- Hartshorn, K., Hovius, N., Dade, W. B., and Slingerland, R. L.: Climate-driven bedrock incision in an active mountain belt, *Science*, 297, 2036–2038, doi:10.1126/science.1075078, 2002.
- Hodge, R. A., Hoey, T. B., and Sklar, L. S.: Bed load transport in bedrock rivers: The role of sediment cover in grain entrainment, translation, and deposition, *J. Geophys. Res.*, 116, F04028, doi:10.1029/2011JF002032, 2011.
- Howard, A. D.: A detachment-limited model of drainage basin evolution, *Water Resour. Res.*, 30, 2261–2285, doi:10.1029/94WR00757, 1994.
- Howard, A. D. and Kerby, G.: Channel changes in badlands, *Geol. Soc. Am. Bull.*, 94, 739–752, doi:10.1130/0016-7606(1983)94<739:CCIB>2.0.CO;2, 1983.
- Howard, A. D., Dietrich, W. E., and Seidl, M. A.: Modeling fluvial erosion on regional to continental scales, *J. Geophys. Res.*, 99, 13971–13986, 1994.

- Inoue, T., Izumi, N., Shimizu, Y., and Parker, G.: Interaction among alluvial cover, bed roughness, and incision rate in purely bedrock and alluvial-bedrock channel, *J. Geophys. Res.-Earth*, 119, 2123–2146, doi:10.1002/2014JF003133, 2014.
- Jacobs, F. and Hagmann, M.: Sediment bypass tunnel Runcahez: Invert abrasion 1995–2014, in: *Proc. First International Workshop on Sediment Bypass Tunnels, VAW-Mitteilungen 232*, edited by: Boes, R. M., Tech. rep., Laboratory of Hydraulics, Hydrology and Glaciology (VAW), ETH Zurich, 2015.
- Johnson, J. P. and Whipple, K. X.: Evaluating the controls of shear stress, sediment supply, alluvial cover, and channel morphology on experimental bedrock incision rate, *J. Geophys. Res.*, 115, F02018, doi:10.1029/2009JF001335, 2010.
- Johnson, J. P. L.: A surface roughness model for predicting alluvial cover and bed load transport rate in bedrock channels, *J. Geophys. Res.-Earth*, 119, 2147–2173, doi:10.1002/2013JF003000, 2014.
- Johnson, J. P. L., Whipple, K. X., Sklar, L. S., and Hanks, T. C.: Transport slopes, sediment cover, and bedrock channel incision in the Henry Mountains, Utah, *J. Geophys. Res.*, 114, F02014, doi:10.1029/2007JF000862, 2009.
- Lague, D.: The stream power river incision model: evidence, theory and beyond, *Earth Surf. Proc. Land.*, 39, 38–61, doi:10.1002/esp.3462, 2014.
- Lague, D., Crave, A., and Davy, P.: Laboratory experiments simulating the geomorphic response to tectonic uplift, *J. Geophys. Res.*, 108, ETG3, doi:10.1029/2002JB001785, 2003.
- Lague, D., Hovius, N., and Davy, P.: Discharge, discharge variability and the bedrock channel profile, *J. Geophys. Res.*, 110, F04006, doi:10.1029/2004JF000259, 2005.
- Lamb, M. P., Dietrich, W. E., and Sklar, L. S.: A model for fluvial bedrock incision by impacting suspended and bed load sediment, *J. Geophys. Res.*, 113, F03025, doi:10.1029/2007JF000915, 2008a.
- Lamb, M. P., Dietrich, W. E., and Venditti, J. G.: Is the critical Shields stress for incipient sediment motion dependent on channel-bed slope?, *J. Geophys. Res.*, 113, F02008, doi:10.1029/2007JF000831, 2008b.
- Mackey, B. H., Scheingross, J. S., Lamb, M. P., and Farley, K. A.: Knickpoint formation, rapid propagation, and landscape response following coastal cliff retreat at the last interglacial sea-level highstand: Kaua'i, Hawai'i, *Geol. Soc. Am. Bull.*, 126, 925–942, doi:10.1130/B30930.1, 2014.
- Miller, J. R.: The influence of bedrock geology on knickpoint development and channel-bed degradation along downcutting streams in south-central Indiana, *J. Geol.*, 99, 591–605, doi:10.1086/629519, 1991.
- Mills, H. H.: Apparent increasing rates of stream incision in the eastern united states during the late cenozoic, *Geology*, 28, 955–957, doi:10.1130/0091-7613(2000)28<955:AIROSI>2.0.CO;2, 2000.
- Nelder, J. A. and Mead, R.: A simplex-method for function minimization, *Comput. J.*, 7, 308–313, 1965.
- Nelson, P. A. and Seminara, G.: Modeling the evolution of bedrock channel shape with erosion from saltating bed load, *Geophys. Res. Lett.*, 38, L17406, doi:10.1029/2011GL048628, 2011.
- Rickenmann, D.: Comparison of bed load transport in torrent and gravel bed streams, *Water Resour. Res.*, 37, 3295–3305, doi:10.1029/2001WR000319, 2001.
- Rickenmann, D. and Koschni, A.: Sediment loads due to fluvial transport and debris flows during the 2005 flood events in Switzerland, *Hydrol. Process.*, 24, 993–1007, doi:10.1002/hyp.7536, 2010.
- Rickenmann, D., Chiari, M., and Friedl, K.: SETRAC – A sediment routing model for steep torrent channels, in: *River Flow 2006*, edited by: Ferreira, R., Alves, C., Leal, G., and Cardoso, A., 843–852, Taylor & Francis Group, London, 2006.
- Rickenmann, D., Turowski, J. M., Fritschi, B., Klaiber, A., and Ludwig, A.: Bedload transport measurements at the Erlenbach stream with geophones and automated basket samplers, *Earth Surf. Proc. Land.*, 37, 1000–1011, doi:10.1002/esp.3225, 2012.
- Rieke-Zapp, D. H., Beer, A., Turowski, J. M., and Campana, L.: IN SITU MEASUREMENT OF BEDROCK EROSION, *Int. Arch. Photogramm. Remote Sens. Spatial Inf. Sci.*, XXXIX-B5, 429–433, doi:10.5194/isprsarchives-XXXIX-B5-429-2012, 2012.
- Scheingross, J. S., Brun, F., Lo, D. Y., Omerdin, K., and Lamb, M. P.: Experimental evidence for fluvial bedrock incision by suspended and bedload sediment, *Geology*, 42, 523–526, doi:10.1130/G35432.1, 2014.
- Schneider, J. M., Turowski, J. M., Rickenmann, D., Hegglin, R., Arrigo, S., Mao, L., and Kirchner, J. W.: Scaling relationships between bed load volumes, transport distances, and stream power in steep mountain channels, *J. Geophys. Res.-Earth*, 119, 533–549, doi:10.1002/2013JF002874, 2014.
- Seidl, M. A. and Dietrich, W. E.: The problem of channel erosion into bedrock, *Catena Supplement*, 23, 101–124, 1992.
- Seidl, M. A., Dietrich, W. E., and Kirchner, J. W.: Longitudinal profile development into bedrock: an analysis of Hawaiian channels, *J. Geol.*, 102, 457–474, 1994.
- Shields, A.: Anwendung der Aehnlichkeitsmechanik und der Turbulenzforschung auf die Geschiebebewegung, *Tech. rep., Mitteilungen der Preussischen Versuchsanstalt fuer Wasserbau und Schiffbau*, 26, 26, 1936 (English translation by W. P. Ott and J. C. van Uchelen), 36 pp., U.S. Dep. of Agric. Soil Conser. Serv. Coop. Lab., Calif., Inst. of Technol., Pasadena, 1936.
- Sklar, L. S. and Dietrich, W. E.: Sediment and rock strength controls on river incision into bedrock, *Geology*, 29, 1087–1090, doi:10.1130/0091-7613(2001)029<1087:SARSCO>2.0.CO;2, 2001.
- Sklar, L. S. and Dietrich, W. E.: A mechanistic model for river incision into bedrock by saltating bed load, *Water Resour. Res.*, 40, W06301, doi:10.1029/2003WR002496, 2004.
- Sklar, L. S. and Dietrich, W. E.: The role of sediment in controlling steady-state bedrock channel slope: implications of the saltation-abrasion incision model, *Geomorphology*, 82, 58–83, doi:10.1016/j.geomorph.2005.08.019, 2006.
- Snyder, N. P., Whipple, K. X., Tucker, G. E., and Merritts, D. J.: Landscape response to tectonic forcing: digital elevation model analysis of stream profiles in the Mendocino triple junction region, northern California, *Geol. Soc. Am. Bull.*, 112, 1250–1263, 2000.
- Snyder, N. P., Whipple, K. X., Tucker, G. E., and Merritts, D. J.: Importance of a stochastic distribution of floods and erosion thresholds in the bedrock river incision problem, *J. Geophys. Res.*, 108, 2117, doi:10.1029/2001JB001655, 2003.
- Stock, J. D. and Montgomery, D. R.: Geologic constraints on bedrock river incision using the stream power law, *J. Geophys. Res.*, 104, 4983–4993, doi:10.1029/98JB02139, 1999.

- Tomkin, J. H., Brandon, M. T., Pazzaglia, F. J., Barbour, J. R., and Willett, S. D.: Quantitative testing of bedrock incision models for the clearwater river, nw, washington state, *J. Geophys. Res.*, 108, 2308, doi:10.1029/2001JB000862, 2003.
- Tucker, G. E. and Slingerland, R. L.: Drainage basin response to climate change, *Water Resour. Res.*, 33, 2031–2047, doi:10.1029/97WR00409, 1997.
- Tucker, G. E. and Whipple, K. X.: Topographic Outcomes predicted by stream erosion models: sensitivity analysis and intermodel comparison, *J. Geophys. Res.*, 107, 2179–2194, doi:10.1029/2001JB000162, 2002.
- Turowski, J. M.: Semi-alluvial channels and sediment-flux-driven bedrock erosion, in: *Gravel Bed Rivers: Processes, Tools, Environments*, Chap. 29, edited by: Church, M., Biron, P., and Roy, A., John Wiley and Sons, Chichester, 401–416, doi:10.1002/9781119952497, 2012.
- Turowski, J. M. and Rickenmann, D.: Tools and cover effects in bedload transport observations in the Pitzbach, Austria, *Earth Surf. Proc. Land.*, 34, 26–37, doi:10.1002/esp.1686, 2009.
- Turowski, J. M., Lague, D., and Hovius, N.: Cover effect in bedrock abrasion: a new derivation and its implication for the modeling of bedrock channel morphology, *J. Geophys. Res.*, 112, F04006, doi:10.1029/2006JF000697, 2007.
- Turowski, J. M., Hovius, N., Hsieh, M. L., Lague, D., and Chen, M. C.: Distribution of erosion across bedrock channels, *Earth Surf. Proc. Land.*, 33, 353–363, doi:10.1002/esp.1559, 2008.
- Turowski, J. M., Badoux, A., and Rickenmann, D.: Start and end of bedload transport in gravel-bed streams, *Geophys. Res. Lett.*, 38, L04401, doi:10.1029/2010GL046558, 2011.
- Turowski, J. M., Boeckli, M., Rickenmann, D., and Beer, A. R.: Field measurements of the energy delivered to the channel bed by moving bedload and links to bedrock erosion, *J. Geophys. Res.*, 118, 2438–2450, doi:10.1002/2013JF002765, 2013.
- Turowski, J. M., Wyss, C., and Beer, A. R.: Grain size effects on energy delivery to the stream bed and links to bedrock erosion, *Geophys. Res. Lett.*, 42, 1775–1780, doi:10.1002/2015GL063159, 2015.
- Valla, P. G., van der Beek, P. A., and Lague, D.: Fluvial incision into bedrock: insights from morphometric analysis and numerical modeling of gorges incising glacial hanging valleys (western alps, france), *J. Geophys. Res.-Earth*, 115, F02010, doi:10.1029/2008JF001079, 2010.
- van der Beek, P. and Bishop, P.: Cenozoic river profile development in the upper Lachlan catchment (SE Australia) as a test of quantitative fluvial incision models, *J. Geophys. Res.*, 108, 2309, doi:10.1029/2002JB002125, 2003.
- Whipple, K. X.: Bedrock rivers and the geomorphology of active orogens, *Annu. Rev. Earth Pl. Sc.*, 32, 151–185, doi:10.1146/annurev.earth.32.101802.120356, 2004.
- Whipple, K. X. and Tucker, G. E.: Dynamics of the stream-power river incision model: implications for height limits of mountain ranges, landscape response timescales, and research needs, *J. Geophys. Res.*, 104, 17661–17674, doi:10.1029/1999JB900120, 1999.
- Whipple, K. X. and Tucker, G. E.: Implications of sediment-flux-dependent river incision models for landscape evolution, *J. Geophys. Res.*, 107, 2039, doi:10.1029/2000JB000044, 2002.
- Whipple, K. X., Hancock, G. S., and Anderson, R. S.: River incision into bedrock: mechanics and relative efficacy of plucking, abrasion, and cavitation, *Geol. Soc. Am. Bull.*, 112, 490–503, doi:10.1130/0016-7606(2000)112<0490:RIIBMA>2.3.CO;2, 2000.
- Whipple, K. X., DiBiase, R. A., and Crosby, B. T.: Bedrock rivers, in: *Treatise in Geomorphology, Methods in Geomorphology*, 9.28, edited by: Switzer, A. and Kennedy, D. M., Elsevier, Amsterdam, 550–573, 2013.
- Wilson, A., Hovius, N., and Turowski, J. M.: Upstream facing convex surfaces: bedrock bedforms produced by fluvial bedload abrasion, *Geomorphology*, 180/181, 187–204, doi:10.1016/j.geomorph.2012.10.010, 2013.
- Wohl, E. E.: Bedrock channel morphology in relation to erosional processes, in: *Rivers Over Rock: Fluvial Processes in Bedrock Channels*, edited by: Tinkler, K. J. and Wohl, E. E., Geophysical Monograph, 107, American Geophysical Union, Washington, DC, 133–151, 1998.
- Wohl, E.: Incised bedrock channels, in: *Incised River Channels*, edited by: Darby, S. E. and Simon, A., chap. 8, 188–218, Wiley, 1999.
- Wohl, E. E., Greenbaum, N., Schick, A., and Baker, V.: Controls on Bedrock Channel Incision along Nahal Paran, Israel, *Earth Surf. Proc. Land.*, 19, 1–13, doi:10.1002/esp.3290190102, 1994.
- Yager, E. M., Dietrich, W. E., Kirchner, J. W., and McArdeall, B. W.: Patch dynamics and stability in steep, rough streams, *J. Geophys. Res.*, 117, F02010, doi:10.1029/2011JF002253, 2012a.
- Yager, E. M., Dietrich, W. E., Kirchner, J. W., and McArdeall, B. W.: Prediction of sediment transport in step-pool channels, *Water Resour. Res.*, 48, W01541, doi:10.1029/2011WR010829, 2012b.
- Zhang, L., Parker, G., Stark, C. P., Inoue, T., Viparelli, E., Fu, X., and Izumi, N.: Macro-roughness model of bedrock-alluvial river morphodynamics, *Earth Surf. Dynam.*, 3, 113–138, doi:10.5194/esurf-3-113-2015, 2015.